Original Article

Endovaginal coil for pelvic high-resolution magnetic resonance imaging of cervical cancer: a preliminary parameter optimization study

Ke Zhang[1,2], Bin Yu[3], Mingmei Tang[1,2], Yingyuan Li[1,4], Meixian Wu[1,4], Fajin Lv[1,3]

[1]State Key Laboratory of Ultrasound in Medicine and Engineering, College of Biomedical Engineering, Chongqing Medical University, Chongqing, China; [2]Chongqing Key Laboratory of Biomedical Engineering, Chongqing Medical University, Chongqing, China; [3]Department of Radiology, the First Affiliated Hospital of Chongqing Medical University, Chongqing, China; [4]Department of Radiology, Liuzhou Maternity and Child Healthcare Hospital, Liuzhou, China

Contributions: (I) Conception and design: All authors; (II) Administrative support: B Yu, F Lv; (III) Provision of study materials or patients: K Zhang, B Yu, F Lv; (IV) Collection and assembly of data: K Zhang; (V) Data analysis and interpretation: K Zhang, M Tang; (VI) Manuscript writing: All authors; (VII) Final approval of manuscript: All authors.

Correspondence to: Fajin Lv, MD. State Key Laboratory of Ultrasound in Medicine and Engineering, College of Biomedical Engineering, Chongqing Medical University, Chongqing 400016, China; Department of Radiology, the First Affiliated Hospital of Chongqing Medical University, No. 1 Youyi Road, Yuzhong District, Chongqing 400016, China. Email: fajinlv@163.com.

Background: The diagnosis of early-stage cervical cancer through conventional magnetic resonance imaging (MRI) remains challenging, highlighting a greater need for pelvic high-resolution MRI (HR MRI). This study used our research team's endovaginal coil imaging to optimize scanning parameters and aimed to achieve HR MRI of the pelvis and determine its clinical value.

Methods: Fifty participants were recruited prospectively for this cross-sectional study conducted at the First Affiliated Hospital of Chongqing Medical University from January 2023 to November 2023. Initially, 10 volunteers requiring pelvic imaging diagnosis underwent pelvic MRI with the endovaginal coil combined with a conventional external array coil to test and optimize the scanning parameters. Subsequently, 40 patients who were highly suspected or diagnosed with cervical cancer were randomly assigned to undergo an initial pelvic scan with an external array coil with subsequent examinations of both the conventional coil and the endovaginal coil. Two experienced radiologists performed quantitative analyses, measuring signals and calculating the signal-to-noise ratio (SNR), contrast-to-noise ratio (CNR), and contrast (C). They also conducted qualitative analyses, evaluating imaging artifacts, anatomical structures, and overall image quality. The paired sample *t*-test and Wilcoxon rank-sum test were conducted to compare the statistical differences between the two sets of images, while the intraclass correlation coefficient (ICC) and Kappa consistency tests were used to assess the measurement and scoring consistency between the two radiologists.

Results: The optimized endovaginal images had higher mean SNR, CNR, and C values (18.62±7.85, 16.04±7.72, and 0.73±0.11, respectively) compared to the conventional images (6.77±2.36, 4.47±2.05, and 0.47±0.12, respectively). Additionally, the ratings for imaging artifacts, anatomical structures, and overall quality of the endovaginal images were all 4 [interquartile range (IQR) 4, 4]; meanwhile, the conventional images scored lower with ratings of 4 (IQR 3, 4), 3 (IQR 3, 3), and 3 (IQR 3, 3) for SNR, CNR, and C, respectively. All analysis results underwent paired-sample *t*-tests or Wilcoxon rank-sum tests between the two groups, yielding a P value <0.001. The optimized endovaginal images also showed improved resolution with a reconstructed voxel size of 0.11 mm^3, and HR MRI was successfully achieved. The ICC values for the measurements were 0.914, 0.947, and 0.912, respectively, and for the ratings, the measurement was 0.923, indicating excellent consistency between the two physicians (ICC/Kappa value between 0.85 and 1.00).

Conclusions: Endovaginal technology, which provides precise clinical information for the diagnosis of cervical cancer, provides straightforward operation and exceptional imaging quality, making it highly suitable for expanded clinical use.

Keywords: Endovaginal coil; high-resolution magnetic resonance imaging (HR MRI); cervical cancer

Submitted Dec 01, 2023. Accepted for publication Apr 03, 2024. Published online May 24, 2024.
doi: 10.21037/qims-23-1718
View this article at: https://dx.doi.org/10.21037/qims-23-1718

Introduction

In recent years, several guidelines (1) and studies (2-4) have emphasized the crucial importance of accurately assessing the depth of infiltration and invasion in cervical intraepithelial neoplasia (CIN) and cervical cancer for early diagnosis and treatment, as it is essential for the survival and prognostic quality of life of patients. Pelvic magnetic resonance imaging (MRI) is the optimal imaging examination method for cervical cancer (3). It aids in detecting lesions, determining size and location, and displaying the depth of lesions invading the cervical stroma. Additionally, it helps ascertain whether lesions are confined to the cervix, parametrium, or pelvic wall. Pelvic MRI provides an important foundation for pretreatment characterization and staging in patients with early-stage cervical cancer (5,6). However, when using the conventional external array coil (this is referred to as the *conventional coil*), the clinical findings of early-stage cervical cancer are inadequately visualized in the MRI images, and the image resolution truly cannot meet diagnostic requirements, particularly for tumors below stage IB1 and smaller than 2 cm (4). The clinical situation leads to a challenging scenario for early diagnosis, highlighting a greater need for pelvic high-resolution MRI (HR MRI).

It has been confirmed that placing the receiver coil closer to the region of interest (ROI) results in higher spatial resolution and signal-to-noise ratio (SNR), thereby improving image quality (7,8). Therefore, the internal MRI endovaginal coil may offer a more promising technique for pelvic HR MRI. It is well known that an efficient apparatus necessitates a pairing with the appropriate scanning parameters to yield higher image quality. Thus, in this study, we applied endovaginal coil imaging—designed in collaboration with our research team—and optimized the scanning parameters, and compared this with conventional pelvic MRI. The goal was to demonstrate the clinical usability of the endovaginal coil from both quantitative and qualitative perspectives and to determine its value for clinical application. We present this article in accordance with the STROBE reporting checklist (available at https://qims.amegroups.com/article/view/10.21037/qims-23-1718/rc).

Methods

Participants

This single-center, prospective, cross-sectional study was conducted in accordance with the Declaration of Helsinki (as revised in 2013) and was approved by the Ethics Committee of the First Affiliated Hospital of Chongqing Medical University (No. 2023-400). Informed consent was obtained from all participants. In total, 50 participants were recruited at the First Affiliated Hospital of Chongqing Medical University from January 2023 to November 2023, and 10 volunteers requiring pelvic imaging diagnosis were randomly selected by the technologist. Subsequently, 40 patients who were highly suspected or diagnosed with cervical cancer were randomly selected. This study included participants who were not experiencing vaginal bleeding, had not undergone uterine or cervical surgery, had provided informed consent, and demonstrated a willingness to cooperate with follow-up. The exclusion criteria were the presence of lesions involving the vagina, contraindications to magnetic resonance examination, and the presence exhibiting significant imaging artifacts due to metal or motion.

Imaging method and sequence parameters

T2-weighted (T2-W) turbo spin echo (TSE) axial plan images were acquired for endovaginal sequence parameter optimization in 10 volunteers. When stable imaging without significant artifacts was achieved in the volunteers, the patients were enrolled in the study.

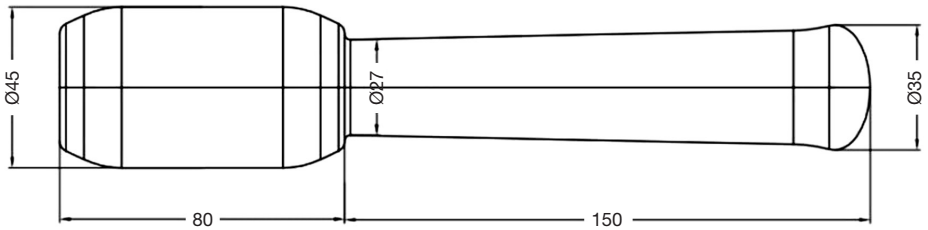

Figure 1 Design diagram of the endovaginal coil. The measurements presented are in millimeters.

Pelvic MRI scans of the patients were performed on a 3.0 T MRI device (MAGNETOM Skyra, Siemens Healthineers, Germany). The conventional scan was initiated with participants in a supine position, with their feet first, and their body aligned with the examination table. After the participant's pelvic region was aligned with the center of the conventional coil and the laser positioning line of the MRI device, the examination table was advanced into the magnet. Images from conventional scans were categorized in the conventional group. Subsequently, an endovaginal coil scan was conducted with the conventional coil being retained. The endovaginal coil (*Figure 1*), shielded with two protective layers and coated with ultrasound gel, was inserted vaginally approximately 1–2 cm from the cervix. The laser positioning method was consistent with the conventional scan. Images from the endovaginal scan were included in the endovaginal group. In both scan types, the scanning localization lines were oriented vertically to the cervix's longitudinal axis. The scan parameters are detailed in *Table 1*.

Imaging analysis

Two diagnostic physicians, with 10 and 6 years of experience in pelvic magnetic resonance diagnostics, respectively, blindly assessed images from both the conventional and endovaginal groups quantitatively and qualitatively using the syngo.via postprocessing workstation (Siemens Healthineers).

Quantitative analysis

On the corresponding axial images of both groups, ROIs were delineated for measurements (*Figure 2*). Consistent ROI size and shape were ensured using a copy-paste method for both groups from the same patient, with an interpatient error in the ROI area of less than 0.01 cm^2. For measuring the signal intensity (SI) of lesions, a circular ROI with an area of 0.2 cm^2 was placed at the homogeneous cervical lesion signal level. For measuring the SI of the piriformis, a circular ROI with an area of 0.3 cm^2 was placed at the homogeneous piriformis signal level. For measuring the standard deviation (SD) of the myometrium, a circular ROI with an area of 0.2 cm^2 was placed at the nonneoplastic uterine or cervical muscle layer with a homogeneous signal level. Due to the nonuniform distribution of the background noise in the images obtained using the parallel acquisition technique (PAT), the SD of the nontumor uterine/cervical myometrial signals was used as the measure of background noise (9). When calculating the contrast-to-noise ratio (CNR) and contrast (C), we used the signal of the piriformis, a smaller muscle in the gluteus, as a reference (9). The formula (9,10) for calculation was as follows:

$$\mathrm{SNR} = \frac{\mathrm{SI}_{\mathrm{lesions}}}{\mathrm{SD}_{\mathrm{myometrium}}} \quad [1]$$

$$\mathrm{CNR}_{\mathrm{lesions\text{-}piriformis}} = \frac{\mathrm{SI}_{\mathrm{lesions}} - \mathrm{SI}_{\mathrm{piriformis}}}{\mathrm{SD}_{\mathrm{myometrium}}} \quad [2]$$

$$\mathrm{C}_{\mathrm{lesions\text{-}piriformis}} = \frac{\mathrm{SI}_{\mathrm{lesions}} - \mathrm{SI}_{\mathrm{piriformis}}}{\mathrm{SI}_{\mathrm{lesions}} + \mathrm{SI}_{\mathrm{piriformis}}} \quad [3]$$

The incremental percentage of the endovaginal group compared to the conventional group was calculated using the following formula:

$$\text{Incremental percentage} = \frac{\mathrm{Mean}_{\mathrm{endovaginal}} - \mathrm{Mean}_{\mathrm{convertional}}}{\mathrm{Mean}_{\mathrm{convertional}}} \times 100\% \quad [4]$$

Qualitative analysis

The subjective evaluation included a 5-point Likert scale (11) (1, nondiagnostic; 2, poor; 3, moderate; 4, good; 5, excellent) to assess image artifacts, anatomical structures, and overall quality. Image artifacts included motion artifacts from respiratory and intestinal peristalsis; anatomical structures included cervical canal morphology, mucosal

Table 1 Comparison of the scanning parameters

Parameter	Conventional group	Endovaginal group
Sequence	TSE	TSE
Plane	Axial	Axial
Coil	External array coil	Endovaginal coil combined with external array coil
TR (ms)	3,200	2,000
TE (ms)	88	88
Slice thickness (mm)	3	2
FOV (mm)	200	180
Matrix	256×256	384×384
Phase oversampling (%)	100	60
Averages	1	2
Flip angle (deg)	160	160
PAT	GRAPPA	GRAPPA
Accel. factor PE	2	2
Reference scan mode	Integrated	Self-calibration
Turbo factor	18	18
Interpolation	On	On
Acquisition voxel size (mm^3)	1.83 (0.78×0.78×3)	0.44 (0.47×0.47×2)
Reconstruction voxel size (mm^3)	0.46 (0.39×0.39×3)	0.11 (0.23×0.23×2)
Acquisition time	1 min 44 s	2 min 30 s

TSE, turbo spin echo; TR, repetition time; TE, echo time; FOV, field of view; PAT, parallel acquisition technique; GRAPPA, generalized autocalibrating partially parallel acquisitions; Accel. factor PE, acceleration factor in the phase encoding direction.

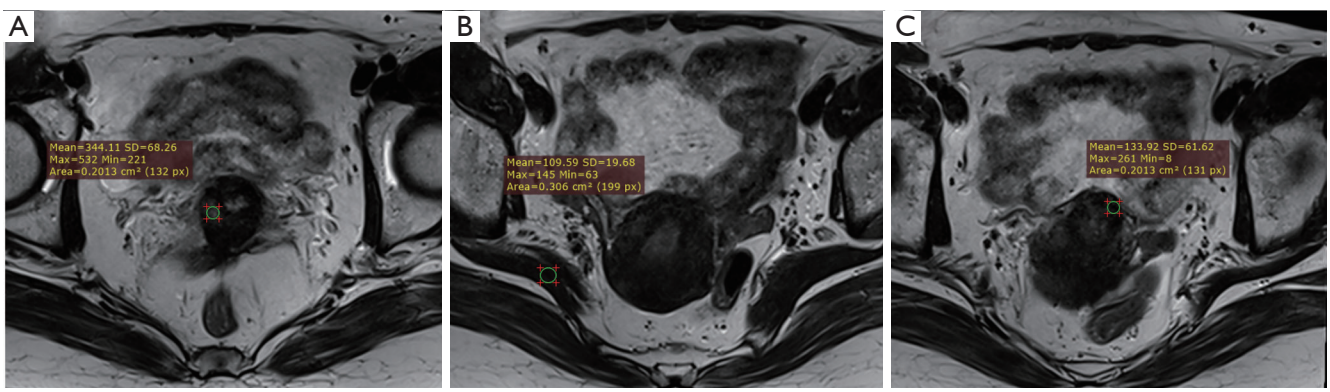

Figure 2 Methods for delineating the ROI. The green circle in the figure represents the ROI area, and the rectangle contains the ROI information. (A) Measurement of SI lesions, with an ROI area of 0.2 cm^2. (B) Measurement of $SI_{piriformis}$, with an ROI area of 0.3 cm^2. (C) Measurement of $SD_{myometrial}$, with an ROI area of 0.2 cm^2. SD, standard deviation; ROI, region of interest; SI, signal intensity.

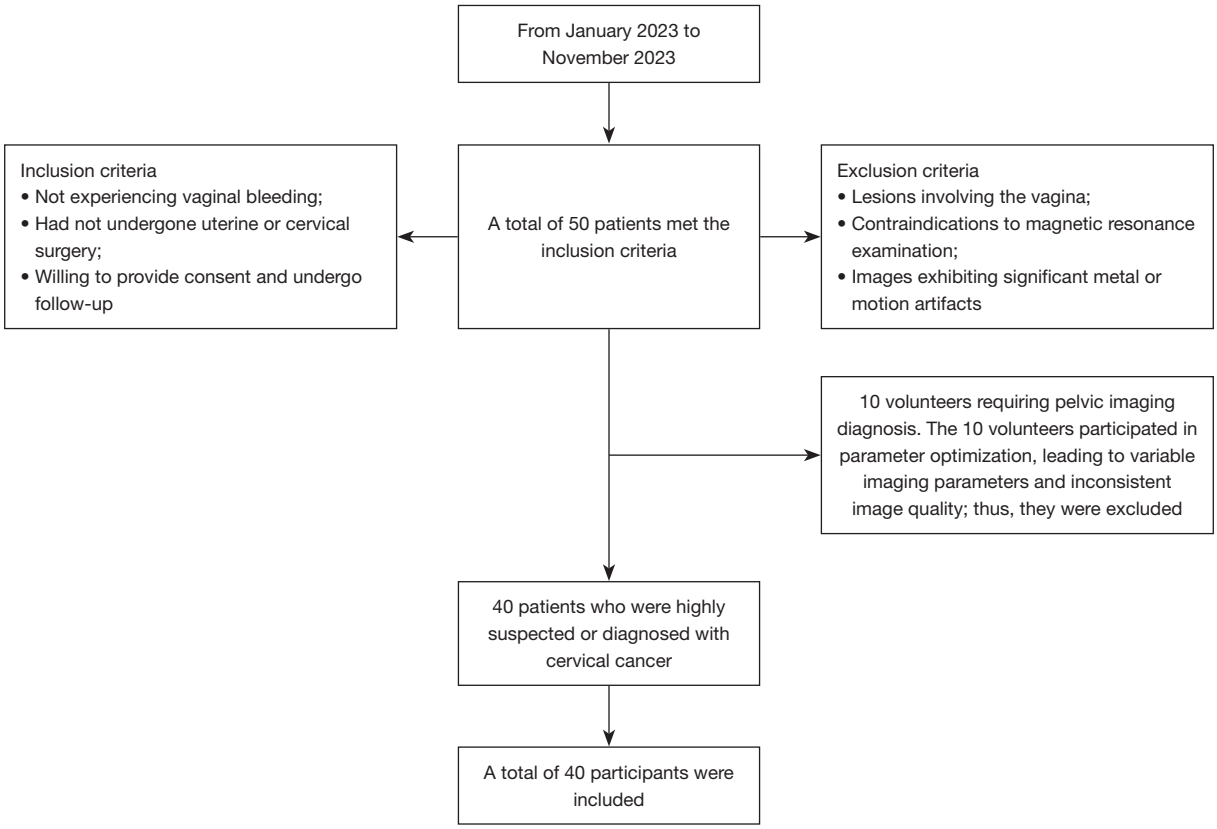

Figure 3 Flowchart of patient selection.

layers, stromal layer, myometrial layers, and cervical margins; and overall quality included factors such as image uniformity, resolution, and SNR. Images with a score of 2 or less were excluded.

Statistical analysis

All statistical tests were performed using SPSS 27 (IBM Corp., Armonk, NY, USA). Quantitative data are expressed as $\bar{x}\pm s$, representing the mean and SD, and were compared with a paired-sample *t*-test; qualitative data are expressed as the median and interquartile range and were compared with a paired-sample Wilcoxon rank sum test. All hypothesis testing was conducted using two-sided tests, with the significance level α set at 0.05. A P value below 0.05 was considered statistically significant. Consistency tests, including the intraclass correlation coefficient (ICC) for measurements between the two diagnosticians and the kappa test for scoring results were performed. Kappa or ICC values below 0.40 indicated poor agreement, 0.4 to 0.54 indicated weak agreement, 0.55 to 0.69 indicated moderate agreement, 0.70 to 0.84 indicated good agreement, and 0.85 to 1.00 indicated excellent agreement (12).

Results

Scans of 50 participants were performed at the First Affiliated Hospital of Chongqing Medical University from January 2023 to November 2023. Among the 50 participants recruited, only 10 participated in parameter optimization and adjustment, leading to variable imaging parameters and inconsistent image quality. As a result, subsequent quantitative and qualitative analyses were not performed (*Figure 3*). Forty participants were included, with a mean volume of 7.95±7.20 cm^3 (range, 0.14 to 25.62 cm^3) and a mean age of 49.78±8.71 years (range, 26 to 70 years). The participants had various diagnoses, including 5 cases of high-grade squamous intraepithelial lesion (HSIL), 7 cases of cervical cancer stage Ia, 8 cases of stage Ib, 12 cases of stage IIa, 4 cases of stage IIb, 3 cases of stage III, and 1 case

Table 2 Clinical and demographic characteristics of the patients

Patient information	Value
Gender (female)	40
Age (years)	49.78±8.71 (26 to 70)
Tumor volume (cm^3)	7.95±7.20 (0.14 to 25.62)
Degree of lesions	
HSIL	5
Ia	7
Ib	8
IIa	12
IIb	4
III	3
IV	1
Pathological classification	
Cervical squamous cancer	22
Cervical adenocarcinoma	10
Small cell neuroendocrine carcinoma	3

The data are presented as mean ± standard deviation (range) or n. HSIL, high-grade squamous intraepithelial lesion.

of stage IV. There were 22 cases of cervical squamous cancer, 10 cases of cervical adenocarcinoma, and 3 cases of small-cell neuroendocrine carcinoma (*Table 2*). All were successfully prospectively recruited for assessment with the conventional coil and subsequently subjected to endovaginal HR MRI.

The optimized endovaginal images showed improved resolution with an acquisition voxel size of 0.44 mm^3 and a reconstructed voxel size of 0.11 mm^3, and HR MRI was successfully achieved (*Table 1*).

Quantitative analysis

The quantitative data in each group followed a normal distribution (*Table 3*). The P values of SNR, CNR, and C in both groups were all less than 0.001, indicating that the differences were statistically significant (P<0.05) (*Table 4*). The ICC values measured by the two diagnostic physicians for the SI_{lesion}, $SI_{piriformis}$, and $SD_{myometrium}$ were 0.914, 0.947, and 0.912, respectively, indicating excellent consistency (ICC between 0.85 and 1.00), and the differences were statistically significant with P<0.001. The SNR, CNR, and C in the endovaginal group showed significant improvement compared to the conventional group (*Figure 4*, *Table 4*). The

Table 3 Normal distribution of quantitative data and qualitative scores

Statistic	SNR	CNR	C	Imaging artifacts	Anatomic structure	Overall quality
Z value	0.953	0.945	0.971	0.873	0.650	0.682
Sig	0.097	0.052	0.383	<0.001	<0.001	<0.001

SNR, signal-to-noise ratio; CNR, contrast-to-noise ratio; C, contrast; Sig, significance level.

Table 4 Comparison of quantitative and qualitative results between the two groups

Statistical method	Indicator	Conventional group	Endovaginal group	$t^{\dagger}$ value/$Z^{\ddagger}$ value	P value
t-test	SNR	6.77±2.36	18.62±7.85	10.978	<0.001
	CNR	4.47±2.05	16.04±7.72	10.839	<0.001
	C	0.47±0.12	0.73±0.11	14.107	<0.001
Wilcoxon rank-sum test	Imaging artifacts	4 (3, 4)	4 (4, 4)	–3.299	<0.001
	Anatomic structure	3 (3, 3)	4 (4, 4)	–5.685	<0.001
	Overall quality	3 (3, 3)	4 (4, 4)	–5.093	<0.001

The data are presented as: quantitative, mean ± standard deviation or qualitative, median (Q1, Q3). †, the *t*-test statistic is represented by the *t* value; ‡, the rank-sum test statistic is denoted by the *Z* value. SNR, signal-to-noise ratio; CNR, contrast-to-noise ratio; C, contrast.

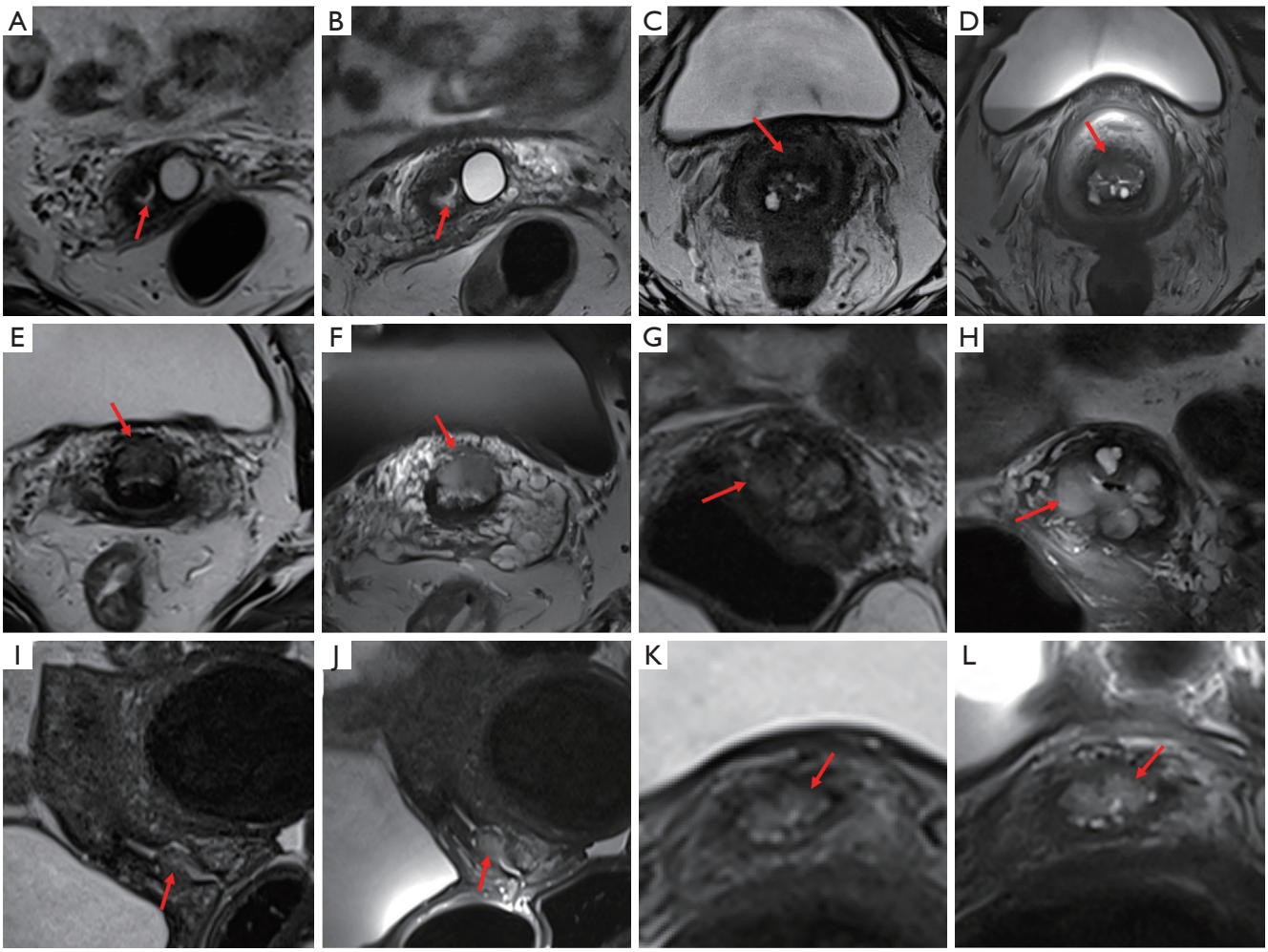

Figure 4 T2-W TSE magnetic resonance imaging images. (A,C,E,G,I,K) Images from the conventional group. (B,D,F,H,J,L) Images from the endovaginal group. (A,B) A 59-year-old patient with CIN III. (A) Only cervical cysts were visible, with no clear indications of cervical cancer-related abnormalities (arrow). (B) There were noticeable abnormal signal patterns with a significant increase (arrow) in the cervical mucosal thickness and precise layering. (C,D) A 50-year-old patient with cervical adenocarcinoma stage Ib1, with the lesion measuring 1.3 cm × 0.7 cm. (C) Poor image contrast made diagnosis difficult (arrow). (D) The anterior lip of the ectocervix plainly showed a piece of nodular T2 lesion with a slightly high signal, indicating an incomplete cervical stromal ring (arrow). (E,F) A 53-year-old patient with low-grade cervical squamous cell carcinoma. (E) The lesions showed no full-layer muscle involvement (arrow), and the conventional image was considered to indicate stage IIa disease. (F) The lesions involved the complete muscle layer with parametrial infiltration (arrow), and the endovaginal coil image was accurately staged as IIb. (G,H) A 51-year-old patient had cervical small cell neuroendocrine carcinoma with *in-situ* stage Ib1 adenocarcinoma. (G) Multiple lesions were visible in the cervix, but the border was imprecise (arrow). (H) Clear lesion boundaries (arrow) with significantly improved image resolution, homogeneity, C, and SNR. (I-L) A 30-year-old patient with cervical adenocarcinoma had a negative immunohistochemistry report. (I,K) The conventional examination revealed a patchy 0.8×0.7 cm abnormal signal pattern in the cervix with unclear boundaries (arrow), casting doubt as to whether it was a tumor. (J,L) The endovaginal examination clearly showed that at the anterior lip of the cervix, the lesion was not penetrating the cervical myometrium but appeared slightly gross. The lesion showed a tendency to break through the cervical junctional zone (arrow), suggesting cervical carcinoma in situ, a conclusion that was further validated via DWI. T2-W, T2-weighted; TSE, turbo spin echo; CIN, cervical intraepithelial neoplasia; C, contrast; SNR, signal-to-noise ratio; DWI, diffusion-weighted imaging.

incremental percentage of the endovaginal group compared to the conventional group was calculated based on the mean values of SNR, CNR, and C presented in *Table 4*. In comparison to that of the conventional group, the SNR of the endovaginal group increased by an average of 175%, the CNR increased by 259%, and C increased by 55%.

Qualitative analysis

Two readers rated all images, with none of the scores being lower than two points. The qualitative data in each group did not follow a normal distribution (*Table 3*). The P values of imaging artifacts, anatomic structure, and overall quality scores between the two groups were all less than 0.001, indicating that the differences were statistically significant ($P<0.05$) (*Table 4*). The kappa value for the subjective ratings of the two diagnostic physicians was 0.923, indicating excellent consistency (kappa between 0.85 and 1.00), and the differences were statistically significant, with $P<0.001$. Imaging artifacts, anatomic structure, and overall quality scores were significantly improved in the endovaginal group compared with the conventional group (*Figure 4*, *Table 4*).

Discussion

Clinical feasibility of the endovaginal coil

In routine clinical pelvic MRI examinations, imaging is typically assisted by a conventional 18-channel external array coil. In adult females, if the pelvis extends 300–350 mm anteriorly or posteriorly, only an area roughly 100–150 mm in diameter remains near the center of the pelvis (13). Small lesions in early-stage cervical cancer may not be adequately visualized on MRI images when conventional coils are used. The accurate range for tumor staging (operable *vs.* advanced disease) determined by clinical findings through MRI is only 75% to 96% (14). The current clinical demands call for HR imaging in pelvic MRI. In 1997, a study confirmed the superior visualization of pelvic floor structures with the use of the endovaginal coil compared to the use of conventional coil (15). In recent two decades, numerous studies (16-23) on the endovaginal coil have predominantly used the 37-mm ring-design solenoidal receiver coil reported in 1996 (24) and 1999 (8). Typically, this coil is inserted into the vaginal cavity during scans, and a conventional coil is concurrently placed to enhance pelvic muscle signals. The synergistic use of these two coils consistently yields superior imaging results (16). However, this coil type has commonly encountered issues: a relatively simple coil design with limited windings; susceptibility artifacts; difficulty in the operation by the radiographer, such as the requirement for a vaginal speculum and external fixation; and poor patient comfort. Furthermore, a new endovaginal coil design intended for radiotherapy, released in 2021, has faced challenges stemming from outdated equipment and a lack of *in vivo* imaging validation (25). With fewer teams seeking to optimize endovaginal coils, there remains ample room for improvement in the design and utilization of this technology. Related studies have revealed issues with the coil's design and usage, as well as variations in imaging equipment and scanning parameters, hindering the stable generation of high-quality images. Therefore, despite the long research history of endovaginal coils, widespread clinical adoption remains elusive.

The endovaginal coil used in this study is an 8-channel intracavitary coil designed by our research team. It detects tissue signals in the magnetic field emitted after excitation by the MRI system through the inductance and capacitance (LC) resonance loop. It is made of environmentally friendly polycarbonate, has no proton signals, and meets safety standards. The adjustable probe section and independent multiangle leg support enhance patient comfort and applicability for cervix imaging in different positions. Moreover, the combined endovaginal coil with optimized sequence parameters improves imaging stability and quality. In the future, our team's endovaginal coil will primarily serve to diagnose early-stage cervical cancer. However, this study examined a diverse range of patients of cervical cancer with different stages and classifications rather than solely focusing on early-stage cases. The aim was to showcase the broad applicability of the endovaginal coil and optimized sequences, ensuring that the sequences do not produce superfluous artifacts due to tumor size or type.

Effect of parameters on image quality

In this study, key parameters such as repetition time (TR), slice thickness, field of view (FOV), etc., were optimized, resulting in a significant and stable improvement in image quality and resolution with the endovaginal coil. The SNR of the endovaginal group increased by an average of 175%, the CNR increased by 259%, and C increased by 55% compared to the conventional group. Due to the limited sample size, the aforementioned percentage data should be regarded solely as supplementary evidence to support the conclusions of this study.

Reduction in scan time

The endovaginal coil used in this study can support the PAT, and both the conventional sequence and the endovaginal sequence used the generalized autocalibrating partially parallel acquisition (GRAPPA) parallel acquisition mode to achieve HR imaging with a small FOV (26). However, there was a difference in the application of reference scan modes in the two groups. The conventional sequence adopted the integrated acquisition mode, meaning that the acquisition phase-encoded reference lines and other phase-encoded lines in K-space are simultaneously acquired. This mode is calibrated quickly, and the extra center lines can increase the SNR of the image. In C, the endovaginal sequence used the self-calibration acquisition mode, leveraging K-space data acquired at different times for mutual calibration. This mode can reduce scanning time while eliminating the need for the additional acquisition of central K-space lines and significantly mitigating sensitivity to motion (27,28). Phase oversampling is an MRI technique that symmetrically increases the sampling range in the phase-encoding direction. This technique can help prevent aliasing artifacts and can also reduce scan time (29,30). We reduced phase oversampling from 100% to 60%, resulting in a 32-second reduction in scan time while maintaining image quality.

Finally, the imaging time for the endovaginal T2-W TSE sequence was 2 minutes and 30. Although this is longer than the imaging time for the conventional group, the improvement in image quality is invaluable and considerably shorter compared to the 4 minutes reported by Downey *et al.* (16). Overall, it is more conducive to clinical promotion and patient acceptance.

Improvement in resolution

To enhance resolution, reducing the FOV is an option; however, an excessively small FOV may lead to alias artifacts (30). In this study, we set the FOV to 180 mm, which still falls within the range of a small FOV for the imaging of human participants (31). This can provide more pelvic information and maximize resolution without causing alias artifacts. The slice thickness of the endovaginal sequence was also reduced to 2 mm, improving resolution (32), and the tradeoff of decreased SNR remains acceptable for overall image quality. Magnetic resonance interpolation is a K-space-based zero-filling technique that effectively enhances image spatial resolution (33). This method increases the sampled points in the frequency direction to boost the frequency encoding steps.

The acquisition resolution for conventional coil images was 0.78×0.78×3 mm, and the reconstruction resolution was 0.39×0.39×3 mm; meanwhile, the acquisition resolution for endovaginal coil images was 0.47×0.47×2 mm, and the reconstruction resolution was 0.23×0.23×2 mm. The resolution of the endovaginal coil images was significantly higher than that of the conventional coil images. In studies reporting high image quality, such as that by Downey *et al.* (16) and Wormald *et al.* (23), a 37-mm ring-design solenoidal receiver coil on 3.0T MRI was applied, the acquisition resolution for endovaginal coil images was 0.42×0.42×2 mm, and the reconstructed resolution was 0.35×0.35×2 mm. In comparison, our study achieved a noticeable resolution improvement under the same slice thickness and a larger FOV.

Limitations and prospects

Currently, the endovaginal coil is nonbendable; therefore, for the small portion of patients who have a very narrow angle between the uterus and cervix, the improvement in image quality using the endovaginal coil may not be substantial, but it is still superior to conventional imaging. We observed a few slight high-signal artifacts in the upper 1–2 planes near the top of the coil. Currently, this type of high signal artifact can only be mitigated by optimizing the endocoil's placement to minimize its impact on the image. We found that positioning the coil 1–2 cm from the cervix is optimal, preventing both high-signal artifacts and a reduction in image SI caused by the coil being too far from the cervix. To position the coil correctly, a T2-W sagittal half-Fourier acquisition single-shot turbo spin echo (HASTE) sequence can be added before the T2 axial TSE sequence to serve as a visual guide.

Our study involved acquiring pelvic plain axial images using the conventional coil alone and in combination with the endovaginal coil. With proper coil placement and optimized sequence application, the endovaginal T2 axial plain images can be expected to surpass conventional T2 axial plain images for comprehensively evaluating the entire pelvic cavity in the future. The Results section of this study demonstrates that the implementation of endovaginal coil intervention facilitates the detection of imperceptible lesions on conventional images (*Figure 4A*) and improves the accuracy of cervical cancer staging (*Figure 4C*). In future clinical research and application, the endovaginal coil can be further leveraged to obtain additional sagittal, coronal, diffusion-weighted imaging (DWI), or C-enhanced scans based on this experimental foundation. This will enable

a more thorough investigation into the impact of this technology on cervical cancer staging and treatment.

Conclusions

Using the endovaginal coil with appropriate scanning parameters consistently produces images with higher resolution, SNR, CNR, and C compared to those obtained using the conventional coil. The endovaginal technology, which provides precise clinical information for the diagnosis of cervical cancer, demonstrates a straightforward operation and exceptional imaging quality, making it highly valuable for clinical application. The endovaginal coil represents an effective technical support tool for achieving pelvic HR MRI.

Acknowledgments

Funding: This work was supported by the State Key Laboratory of Ultrasound in Medicine and Engineering (grant No. 2022KFKT005 to K.Z.).

Footnote

Reporting Checklist: The authors have completed the STROBE reporting checklist. Available at https://qims.amegroups.com/article/view/10.21037/qims-23-1718/rc

Conflicts of Interest: All authors have completed the ICMJE uniform disclosure form (available at https://qims.amegroups.com/article/view/10.21037/qims-23-1718/coif). K.Z. reports funding from the Foundation of State Key Laboratory of Ultrasound in Medicine and Engineering (No. 2022KFKT005) and the provision of the magnetic resonance equipment and experimental environment from the Department of Radiology, the First Affiliated Hospital of Chongqing Medical University. The other authors have no conflicts of interest to declare.

Ethical Statement: The authors are accountable for all aspects of the work in ensuring that questions related to the accuracy or integrity of any part of the work are appropriately investigated and resolved. This study was conducted in accordance with the Declaration of Helsinki (as revised in 2013) and was approved by the Ethics Committee of the First Affiliated Hospital of Chongqing Medical University (No. 2023-400). Informed consent was obtained from all participants.

References

1. Perkins RB, Guido RS, Castle PE, Chelmow D, Einstein MH, Garcia F, Huh WK, Kim JJ, Moscicki AB, Nayar R, Saraiya M, Sawaya GF, Wentzensen N, Schiffman M; 2019 ASCCP Risk-Based Management Consensus Guidelines Committee. 2019 ASCCP Risk-Based Management Consensus Guidelines for Abnormal Cervical Cancer Screening Tests and Cancer Precursors. J Low Genit Tract Dis 2020;24:102-31.
2. He F, Zu S, Chen X, Liu J, Yi Y, Yang H, Wang F, Yuan S. Preoperative magnetic resonance imaging criteria for predicting lymph node metastasis in patients with stage IB1-IIA2 cervical cancer. Cancer Med 2021;10:5429-36.
3. Mao L, Zhang X, Chen T, Li Z, Yang J. High-resolution reduced field-of-view diffusion-weighted magnetic resonance imaging in the diagnosis of cervical cancer. Quant Imaging Med Surg 2023;13:3464-76.
4. Zhang Z, Zhang C, Xiao L, Zhang S. Diagnosis of Early Cervical Cancer with a Multimodal Magnetic Resonance Image under the Artificial Intelligence Algorithm. Contrast Media Mol Imaging 2022;2022:6495309.
5. Peppercorn PD, Jeyarajah AR, Woolas R, Shepherd JH, Oram DH, Jacobs IJ, Armstrong P, Lowe D, Reznek RH. Role of MR imaging in the selection of patients with early cervical carcinoma for fertility-preserving surgery: initial experience. Radiology 1999;212:395-9.
6. Abdul-Latif M, Tharmalingam H, Tsang Y, Hoskin PJ. Functional Magnetic Resonance Imaging in Cervical Cancer Diagnosis and Treatment. Clin Oncol (R Coll Radiol) 2023;35:598-610.
7. Gopalan K, Maravilla J, Mendelsohn J, Arias AC, Lustig M. Vacuum formed coils for MRI. Magn Reson Med 2023;89:1684-96.
8. Gilderdale DJ, deSouza NM, Coutts GA, Chui MK, Larkman DJ, Williams AD, Young IR. Design and use of internal receiver coils for magnetic resonance imaging. Br J Radiol 1999;72:1141-51.

9. Hori M, Kim T, Onishi H, Ueguchi T, Tatsumi M, Nakamoto A, Tsuboyama T, Tomoda K, Tomiyama N. Uterine tumors: comparison of 3D versus 2D T2-weighted turbo spin-echo MR imaging at 3.0 T--initial experience. Radiology 2011;258:154-63.
10. Janssen NNY, Ter Beek LC, Loo CE, Winter-Warnars G, Lange CAH, van Loveren M, Alderliesten T, Sonke JJ, Nijkamp J. Supine Breast MRI Using Respiratory Triggering. Acad Radiol 2017;24:818-25.
11. Lane BF, Vandermeer FQ, Oz RC, Irwin EW, McMillan AB, Wong-You-Cheong JJ. Comparison of sagittal T2-weighted BLADE and fast spin-echo MRI of the female pelvis for motion artifact and lesion detection. AJR Am J Roentgenol 2011;197:W307-13.
12. Schober P, Mascha EJ, Vetter TR. Statistics From A (Agreement) to Z (z Score): A Guide to Interpreting Common Measures of Association, Agreement, Diagnostic Accuracy, Effect Size, Heterogeneity, and Reliability in Medical Research. Anesth Analg 2021;133:1633-41.
13. Langer JE, Oliver ER, Lev-Toaff AS, Coleman BG. Imaging of the female pelvis through the life cycle. Radiographics 2012;32:1575-97.
14. Bourgioti C, Chatoupis K, Moulopoulos LA. Current imaging strategies for the evaluation of uterine cervical cancer. World J Radiol 2016;8:342-54.
15. Tan IL, Stoker J, Laméris JS. Magnetic resonance imaging of the female pelvic floor and urethra: body coil versus endovaginal coil. MAGMA 1997;5:59-63.
16. Downey K, Attygalle AD, Morgan VA, Giles SL, MacDonald A, Davis M, Ind TE, Shepherd JH, deSouza NM. Comparison of optimised endovaginal vs external array coil T2-weighted and diffusion-weighted imaging techniques for detecting suspected early stage (IA/IB1) uterine cervical cancer. Eur Radiol 2016;26:941-50.
17. Downey K, Shepherd JH, Attygalle AD, Hazell S, Morgan VA, Giles SL, Ind TE, Desouza NM. Preoperative imaging in patients undergoing trachelectomy for cervical cancer: validation of a combined T2- and diffusion-weighted endovaginal MRI technique at 3.0 T. Gynecol Oncol 2014;133:326-32.
18. Charles-Edwards EM, Messiou C, Morgan VA, De Silva SS, McWhinney NA, Katesmark M, Attygalle AD, DeSouza NM. Diffusion-weighted imaging in cervical cancer with an endovaginal technique: potential value for improving tumor detection in stage Ia and Ib1 disease. Radiology 2008;249:541-50.
19. Charles-Edwards E, Morgan V, Attygalle AD, Giles SL, Ind TE, Davis M, Shepherd J, McWhinney N, deSouza NM. Endovaginal magnetic resonance imaging of stage 1A/1B cervical cancer with A T2- and diffusion-weighted magnetic resonance technique: effect of lesion size and previous cone biopsy on tumor detectability. Gynecol Oncol 2011;120:368-73.
20. Downey K, Riches SF, Morgan VA, Giles SL, Attygalle AD, Ind TE, Barton DP, Shepherd JH, deSouza NM. Relationship between imaging biomarkers of stage I cervical cancer and poor-prognosis histologic features: quantitative histogram analysis of diffusion-weighted MR images. AJR Am J Roentgenol 2013;200:314-20.
21. Downey K, Jafar M, Attygalle AD, Hazell S, Morgan VA, Giles SL, Schmidt MA, Ind TE, Shepherd JH, deSouza NM. Influencing surgical management in patients with carcinoma of the cervix using a T2- and ZOOM-diffusion-weighted endovaginal MRI technique. Br J Cancer 2013;109:615-22.
22. Wormald BW, Doran SJ, Ind TE, D'Arcy J, Petts J, deSouza NM. Radiomic features of cervical cancer on T2- and diffusion-weighted MRI: Prognostic value in low-volume tumors suitable for trachelectomy. Gynecol Oncol 2020;156:107-14.
23. Wormald B, Rodriguez-Manzano J, Moser N, Pennisi I, Ind TEJ, Vroobel K, Attygalle A, Georgiou P, deSouza NM. Loop-Mediated Isothermal Amplification Assay for Detecting Tumor Markers and Human Papillomavirus: Accuracy and Supplemental Diagnostic Value to Endovaginal MRI in Cervical Cancer. Front Oncol 2021;11:747614.
24. deSouza NM, Scoones D, Krausz T, Gilderdale DJ, Soutter WP. High-resolution MR imaging of stage I cervical neoplasia with a dedicated transvaginal coil: MR features and correlation of imaging and pathologic findings. AJR Am J Roentgenol 1996;166:553-9.
25. Alipour A, Viswanathan AN, Watkins RD, Elahi H, Loew W, Meyer E, Morcos M, Halperin HR, Schmidt EJ. An endovaginal MRI array with a forward-looking coil for advanced gynecological cancer brachytherapy procedures: Design and initial results. Med Phys 2021;48:7283-98.
26. Hamilton J, Franson D, Seiberlich N. Recent advances in parallel imaging for MRI. Prog Nucl Magn Reson Spectrosc 2017;101:71-95.
27. Zhang C, Cristobal-Huerta A, Hernandez-Tamames JA, Klein S, Poot DHJ. Autocalibrated parallel imaging reconstruction with sampling pattern optimization for GRASE: APIR4GRASE. Magn Reson Imaging 2020;66:141-51.
28. Arunachalam A, Samsonov A, Block WF. Self-calibrated

GRAPPA method for 2D and 3D radial data. Magn Reson Med 2007;57:931-8.
29. Jang JS, Lee HB, Suh CH, Lee MH. Image quality and acquisition time assessments for phase oversampling in compressed sensing sensitivity encoding: Comparison with conventional SENSE. J Appl Clin Med Phys 2022;23:e13509.
30. Ahmed SY, Hassan FF. Optimizing imaging resolution in brain MRI: understanding the impact of technical factors. J Med Life 2023;16:920-4.
31. Devine C, Gardner C, Sagebiel T, Bhosale P. Magnetic Resonance Imaging in the Diagnosis, Staging, and Surveillance of Cervical Carcinoma. Semin Ultrasound CT MR 2015;36:361-8.
32. Epistatou AC, Tsalafoutas IA, Delibasis KK. An Automated Method for Quality Control in MRI Systems: Methods and Considerations. J Imaging 2020;6:111.
33. Fellner F, Fellner C, Held P, Schmitt R. Comparison of spin-echo MR pulse sequences for imaging of the brain. AJNR Am J Neuroradiol 1997;18:1617-25.

Cite this article as: Zhang K, Yu B, Tang M, Li Y, Wu M, Lv F. Endovaginal coil for pelvic high-resolution magnetic resonance imaging of cervical cancer: a preliminary parameter optimization study. Quant Imaging Med Surg 2024;14(6):3851-3862. doi: 10.21037/qims-23-1718

